

Secular dynamics for curved two-body problems

Connor Jackman*

Abstract

Consider the dynamics of two point masses on a surface of constant curvature subject to an attractive force analogue of Newton's inverse square law, that is under a 'cotangent' potential. When the distance between the bodies is sufficiently small, the reduced equations of motion may be seen as a perturbation of an integrable system. We take suitable action-angle coordinates to average these perturbing terms and describe dynamical effects of the curvature on the motion of the two-bodies.

1 Introduction

As the geometry of constant curvature spaces developed in the 19th century, the mathematical study of mechanical problems in such spaces presented an opportunity to explore variations of familiar themes. In particular, studying the motion of point masses subject to extensions of Newton's usual (flat) inverse square force law to analogous 'curved inverse square laws' was soon undertaken, see e.g. the historical reviews in [6, 8]. Consequently, we speak of *the* curved Kepler problem or *the* curved n -body problem to refer to the mechanics of point masses in a space of constant curvature under such nowadays customary extensions of Newton's inverse square law.

While the curved Kepler problem is quite similar to the flat Kepler problem –both being characterized by their conformance to analogues of Kepler's laws, or super-integrability– there are striking differences between the curved 2-body problem and the usual 2-body problem. Namely, it has long been noticed that the absence of Galilean boosts prohibits straightforward reduction of a curved 2-body problem to a curved Kepler problem. More recently it has been shown –as an application of Morales-Ramis theory in [14], and by numerically exhibiting complicated dynamics in [5]– that the curved 2-body problem, in contrast to the usual 2-body problem, is 'non-integrable': not admitting analytic first integrals independent of the 'obvious' energy and angular momentum integrals. The purpose of this article is to extend standard averaging techniques, long used in celestial mechanics, to these curved 2-body problems. Consequently, we establish and describe new orbits of the curved 2-body problem in a regime of configurations with the two bodies sufficiently close.

When the distance between the two bodies is small, one expects the curvature of the space to have only a slight influence on their motion. Indeed, after a reduction and scaling (prop. 3.5), we find their relative motion governed by a Kepler problem and additional perturbing terms which vanish as the distance between the bodies goes to zero. These perturbing terms represent the obstruction to reducing the curved 2-body problem to a Kepler problem as one would in the flat case. Thus, one may view their relative motion at each instant as approximately along an *osculating conic*: the conic one body would trace around the other if these perturbing terms were ignored. The averaged, or *secular*, dynamics allow us to see how the perturbing terms slowly deform these osculating conics.

The dominant effect of these perturbing terms causes the osculating conics to precess (fig. 4). Our main result, following from a simple application of a KAM theorem [11] and the implicit function theorem, is that many such orbits may be continued when the full perturbation is taken into account:

Theorem. For two sufficiently close bodies in a space of constant curvature, there exist periodic and quasi-periodic orbits of the reduced curved 2-body problem following osculating conics which, in the positive curvature case (resp. negative curvature case), precess in a direction opposite to (resp. the same as) the bodies motion around their osculating conics.

*e-mail: connor.jackman@cimat.mx, Cimat, Guanajuato, Mexico. May 12, 2021

See theorems 1 and 2 below. The lifts of these new quasi-periodic and periodic orbits to the (spherical) curved 2-body problem are depicted in fig. 1.

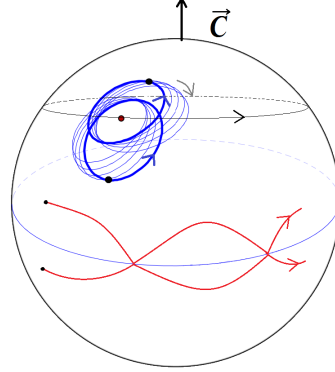


Figure 1: Orbits of two sufficiently close bodies on a sphere with fixed angular momentum \vec{C} (vertical). Approximately, the two bodies (fast) motion is around conic sections which slowly precess in a direction *opposite* to the bodies motion around the conics. The two conics share a focus (located at an approximate ‘center of mass’) lying on a certain latitude (intersection of the sphere by a perpendicular plane to \vec{C}) and the whole system is rotated about the angular momentum axis. As this latitude approaches the equator (the great circle \vec{C}^\perp), the precession rate decreases and the eccentricity of their osculating conics increases. At the equator we find two types of (regularized) periodic collision orbits experiencing no precession: one for which the two bodies bounce perpendicularly to the equator (pictured) and another for which they bounce along an arc aligned with the equator (see rem. B.2). Similar results hold for two bodies in hyperbolic space, with collision orbits occurring for spacelike (or zero) angular momentum values, and the precession occurring in the *same* direction as the bodies motion around the conics.

We will begin (sec. 2) by recalling properties of the curved Kepler problem, defining a system of action-angle coordinates in app. A. The curved 2-body problem admits symmetries by the isometry group of the space of constant curvature, and we next (sec. 3) carry out a Marsden-Weinstein-Meyer reduction to formulate the equations of motion for the reduced curved 2-body problem, then define a scaling of the coordinates (prop. 3.5) allowing us to focus our attention on the dynamics when the two bodies are close relative to the curvature of the space. In sec. 4, we apply a KAM theorem and the implicit function theorem to obtain our main results and then describe the lifting process used to obtain fig. 1.

Remark 1.1. Our results are a natural continuation of the works [4, 5]. In [4], averaging methods were applied to the *restricted* curved 2-body problem using ‘curved Delaunay coordinates’ derived by separation of variables, while the curved 2-body problem was studied in [5] without the use of averaging methods. Here, we apply averaging methods to the curved 2-body problem. Also, in app. A, we outline a different more geometric derivation of these ‘curved Delaunay’ action-angle coordinates. Upon choosing an appropriate representative for the reduction, our methods for determining the averaged dynamics proceed similarly to those applied to the usual 3-body problem in [9], although the setting here is simpler in the sense that we only need to average over one fast angle.

2 Curved Kepler problems

Newton’s ‘ $1/r$ ’ potential may be characterized by either of the following properties:

- it is a (constant multiple) of the fundamental solution of the 3-dimensional laplacian, $\Delta_{\mathbf{R}^3}$
- the orbits of the corresponding central force problem follow Kepler’s laws.

Generalizing these properties to spaces of constant positive (resp. negative) curvature yields ‘ $\cot \varphi$ ’ (resp. ‘ $\coth \varphi$ ’) potentials. We refer to [1] for a discussion of these long established potentials and their properties using central projection (fig. 2), presenting some details here in appendix A. In particular, the curved Kepler problems are super integrable and on the open subset of initial conditions leading to (non-circular) bounded motions we have action-angle coordinates, (L, ℓ, G, g) , where the energy depends only on L (see prop. A.5).

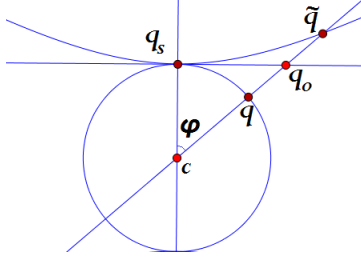


Figure 2: The curved Kepler dynamics –with *fixed* center of attraction or ‘sun’ at q_s – may be characterized by requiring that its *unparametrized* trajectories centrally project to those of the flat Kepler problem in the tangent plane at q_s . Setting $\rho = |cq_s|$, the sphere has curvature $\kappa = 1/\rho^2$ and the hyperboloid (with the restricted Minkowski metric) has curvature $\kappa = -1/\rho^2$. We call $\varphi := \angle(q_s cq)$ (resp. $\tilde{\varphi} := \angle(q_s c \tilde{q})$) measured with the Minkowski inner product the *angular distance* from q to q_s (resp. \tilde{q} to q_s). The distance from q on the sphere to q_s is given by $\rho\varphi$, while the distance from \tilde{q} to q_s on the hyperboloid is given by $\rho\tilde{\varphi}$.

In what follows, we will consider motions of the curved 2-body problem satisfying $\varphi = O(\varepsilon)$ for all time, where ε is a small parameter and $\varphi = \angle(\vec{q}_1, \vec{q}_2)$ is the *angular distance*: the angle between the two bodies on the sphere as measured from the center of the sphere. To avoid repetitive arguments and computations, we will focus on the positive curvature case, remarking at times on analogous results for negative curvature.

3 Curved two body problems

In this section, we will present our reduction of the curved 2-body problem (prop. 3.1), and scaling of the coordinates (prop. 3.5) used to focus on the dynamics when the two bodies are close. We first define the dynamics of the curved 2-body problem on the sphere.

Let S^2 be the sphere of curvature $\kappa = \frac{1}{\rho^2}$, with $\|\cdot\|_\kappa$ the norm given by its constant curvature metric. Consider two point masses,

$$(q_1, q_2) =: q \in (S^2 \times S^2) \setminus \{|\cot \varphi| = \infty\} =: Q,$$

on this sphere of masses $m_1, m_2 > 0$ with φ the angular distance between q_1 and q_2 . Normalize the masses so that $m_1 + m_2 = 1$. We are interested in the Hamiltonian flow on T^*Q of:

$$F := \frac{\|p_1\|_\kappa^2}{2m_1} + \frac{\|p_2\|_\kappa^2}{2m_2} - \frac{m_1 m_2}{\rho} \cot \varphi.$$

The tangential components of the forces are of equal magnitude and directed towards each other along the arc $\widehat{q_1 q_2}$. By letting \vec{q}_j be the position vector of q_j from the center of the sphere, the components of the *angular momentum vector*:

$$\vec{C} := m_1 \vec{q}_1 \times \dot{\vec{q}}_1 + m_2 \vec{q}_2 \times \dot{\vec{q}}_2$$

are first integrals. They correspond to the symmetry by the diagonal action, $(q_1, q_2) \mapsto (gq_1, gq_2)$, of SO_3 on Q . Since $\varphi \neq 0, \pi$ in Q , this SO_3 action on each level set $\{\varphi = \text{cst.}\} \subset Q$ is free and transitive. By choosing a representative configuration (see fig. 3):

$$q^o(\varphi) := (-\rho \sin m_2 \varphi \hat{j} + \rho \cos m_2 \varphi \hat{k}, \rho \sin m_1 \varphi \hat{j} + \rho \cos m_1 \varphi \hat{k}) \quad (1)$$

in each level set of φ we obtain a slice of this group action and have:

$$Q \cong I \times \mathrm{SO}_3, \quad I = (0, \pi) \ni \varphi,$$

such that the SO_3 action is by left multiplication on the second factor.

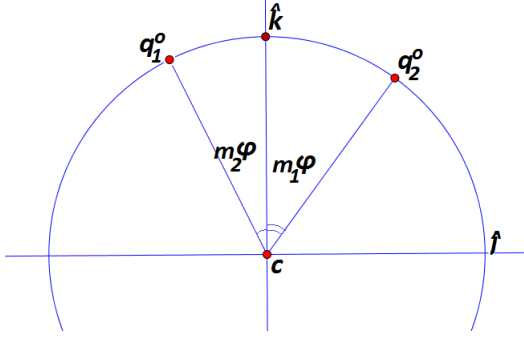


Figure 3: Our choice of representative configuration (eq. (1)). Embed the sphere of radius ρ in \mathbf{R}^3 , centered at the origin and take an orthonormal basis $\hat{i}, \hat{j}, \hat{k}$ of \mathbf{R}^3 . Given $q \in Q$ with angular distance φ between the two bodies, there is a unique element $g \in \mathrm{SO}_3$ with $q = gq^o(\varphi)$.

3.1 Reduced equations of motion

An application of symplectic reduction (see, e.g., [3] App. 5) gives:

Proposition 3.1. Fix the angular momentum $\vec{C} \neq 0$. The reduced 2-body dynamics on a sphere of curvature $\kappa = \frac{1}{\rho^2}$ takes place in $T^*I \times \mathcal{O}_\mu$, where \mathcal{O}_μ is a co-adjoint orbit in \mathfrak{so}_3^* . It is given by the Hamiltonian flow of:

$$F_{red} = Kep_\kappa + \kappa \left(\frac{\|\vec{C}\|^2}{2} - p_\theta^2 \right) + O(\varphi), \quad dp_\varphi \wedge d\varphi + dp_\theta \wedge d\theta,$$

with $|p_\theta| < \|\vec{C}\|$. Here $Kep_\kappa = \frac{p_\varphi^2 + p_\theta^2 / \sin^2 \varphi}{2\rho^2 m} - \frac{m}{\rho} \cot \varphi$, with $m = m_1 m_2$, is the Hamiltonian for a curved Kepler problem.

Proof. We first find the mass weighted metric, $\langle (\vec{v}_1, \vec{v}_2), (\vec{u}_1, \vec{u}_2) \rangle = m_1 \vec{v}_1 \cdot \vec{u}_1 + m_2 \vec{v}_2 \cdot \vec{u}_2$, in terms of our identification $Q \cong I \times \mathrm{SO}_3$ (fig. 3). Since the metric is invariant under left translations, it suffices to determine it at the identity (our representative configurations, q^o , in fig. 3).

Let X_1, X_2, X_3 be the infinitesimal symmetry vector fields generated by rotations about the $\hat{i}, \hat{j}, \hat{k}$ axes. Together with ∂_φ , they frame Q . We compute:

$$\begin{aligned} \langle \partial_\varphi, \partial_\varphi \rangle_{q^o} &= \rho^2 m_1 m_2 & \langle X_1, X_1 \rangle_{q^o} &= m_1 \|\hat{i} \times \vec{q}_1^o\|^2 + m_2 \|\hat{i} \times \vec{q}_2^o\|^2 = \rho^2 \\ \langle X_2, X_2 \rangle_{q^o} &= \rho^2 (m_1 \cos^2 m_2 \varphi + m_2 \cos^2 m_1 \varphi) & \langle X_3, X_3 \rangle_{q^o} &= \rho^2 (m_1 \sin^2 m_2 \varphi + m_2 \sin^2 m_1 \varphi) \\ \langle X_2, X_3 \rangle_{q^o} &= \rho^2 (m_1 \cos m_2 \varphi \sin m_1 \varphi - m_2 \cos m_1 \varphi \sin m_2 \varphi), \end{aligned}$$

all other inner products being zero. In terms of Q 's co-frame, $\{d\varphi, X^j\}$, dual to the above frame, the metric is given by inverting its $\{\partial_\varphi, X_j\}$ matrix representation:

$$\begin{aligned} \langle d\varphi, d\varphi \rangle_{q^o} &= \frac{1}{\rho^2 m_1 m_2} & \langle X^1, X^1 \rangle_{q^o} &= \frac{1}{\rho^2} \\ \langle X^2, X^2 \rangle_{q^o} &= \frac{m_1 \sin^2 m_2 \varphi + m_2 \sin^2 m_1 \varphi}{m_1 m_2 \rho^2 \sin^2 \varphi} & \langle X^3, X^3 \rangle_{q^o} &= \frac{m_1 \cos^2 m_2 \varphi + m_2 \cos^2 m_1 \varphi}{m_1 m_2 \rho^2 \sin^2 \varphi} \\ \langle X^2, X^3 \rangle_{q^o} &= \frac{m_2 \cos m_1 \varphi \sin m_2 \varphi - m_1 \cos m_2 \varphi \sin m_1 \varphi}{m_1 m_2 \rho^2 \sin^2 \varphi}. \end{aligned}$$

We identify $T^*Q \cong T^*I \times (\mathrm{SO}_3 \times \mathfrak{so}_3^*)$ by right translation: $\alpha_g \in T_g^* \mathrm{SO}_3 \mapsto (g, R_g^* \alpha_g)$. In these coordinates, the symplectic lift of SO_3 's left action on Q is given by: $g \cdot (\varphi, p_\varphi, h, \mu) = (\varphi, p_\varphi, gh, Ad_{g^{-1}}^* \mu)$ with associated moment map: $J(\varphi, p_\varphi, g, \mu) = \mu$. The reduced dynamics takes place on the quotient $P_\mu := J^{-1}(\mu)/G_\mu \cong T^*I \times \mathcal{O}_\mu$, realized by: $(\varphi, p_\varphi, g, \mu) \mapsto (\varphi, p_\varphi, Ad_g^* \mu)$. The reduced symplectic form on P_μ is $dp_\varphi \wedge d\varphi + \Omega$, where $\Omega_\nu(ad_\xi^* \nu, ad_\eta^* \nu) = \nu([\xi, \eta])$ is the Kirillov-Kostant form on \mathcal{O}_μ .

By left invariance of the two body Hamiltonian, F , we have: $F(\varphi, p_\varphi, g, \mu) = F(\varphi, p_\varphi, e, Ad_g^*\mu)$, or letting $\nu = Ad_g^*\mu = \nu_j X^j(q^o)$, and $m = m_1 m_2$, we have:

$$F_{red} = \frac{p_\varphi^2}{2m\rho^2} - \frac{m}{\rho} \cot \varphi + \frac{\nu_1^2}{2\rho^2} + \nu_2^2 \frac{m_1 \sin^2 m_2 \varphi + m_2 \sin^2 m_1 \varphi}{2m\rho^2 \sin^2 \varphi} \\ + \nu_3^2 \frac{m_1 \cos^2 m_2 \varphi + m_2 \cos^2 m_1 \varphi}{2m\rho^2 \sin^2 \varphi} + \nu_2 \nu_3 \frac{m_2 \cos m_1 \varphi \sin m_1 \varphi - m_1 \cos m_2 \varphi \sin m_2 \varphi}{m\rho^2 \sin^2 \varphi}. \quad (2)$$

Now, using that $\frac{\sin^2 ax}{\sin^2 x}$ is an analytic function around $x = 0$, with expansion $a^2 + O(x^2)$, and that the $\nu_2 \nu_3$ coefficient is analytic around $\varphi = 0$ of $O(\varphi)$, and $\nu_1^2 + \nu_2^2 + \nu_3^2 = \|\vec{C}\|^2$, we have:

$$F_{red} = \frac{p_\varphi^2}{2m\rho^2} + \frac{\nu_3^2}{2m\rho^2 \sin^2 \varphi} - \frac{m}{\rho} \cot \varphi + \kappa \left(\frac{\|\vec{C}\|^2}{2} - \nu_3^2 \right) + O(\varphi).$$

Finally, recall that the Kirillov-Kostant form is given by $\Omega = dp_\theta \wedge d\theta$ when we parametrize \mathcal{O}_μ -away from the 'poles' $|p_\theta| = \|\vec{C}\|$ -as

$$(\sqrt{\|\vec{C}\|^2 - p_\theta^2} \sin \theta, \sqrt{\|\vec{C}\|^2 - p_\theta^2} \cos \theta, p_\theta) = (\nu_1, \nu_2, \nu_3). \quad (3)$$

□

Remark 3.2. The reduction above may be thought of as a curved analogue of the usual conversion of a flat 2-body problem to a Kepler problem, with the $O(\kappa, \varphi)$ terms representing the obstruction to this equivalence in the curved case. The coordinates (φ, θ) take the role of polar coordinates for the relative position vector, $\vec{q}_1 - \vec{q}_2$, in the flat case, and our choice of representative (fig. 3) corresponds to the role of the center of mass, $m_1 \vec{q}_1 + m_2 \vec{q}_2$, in the flat case.

Remark 3.3. For equal masses, the expression for F_{red} may be simplified by taking $\psi = \varphi/2, p_\psi = 2p_\varphi$. One has: $F_{red} = Kep_\kappa + \frac{\tan \psi}{8\rho} + \kappa \frac{\|\vec{C}\|^2 - p_\theta^2}{2} (1 + (\tan \psi \cos \theta)^2)$, where $Kep_\kappa = \frac{1}{2\rho^2} (p_\psi^2 + \frac{p_\theta^2}{\sin^2 \psi}) - \frac{\cot \psi}{8\rho}$.

Remark 3.4. Reduction has been applied to the curved 2-body problem before, see e.g. [14, 7]. Our choice of representative (fig. 3) was motivated by the mass metric being 'more diagonal', namely requiring: $\langle \partial_\varphi, X_j \rangle = 0$. The reduction in [7], is based on a different representative configuration, namely by taking $q_1^o = \hat{k}, q_2^o = \rho \sin \varphi \hat{j} + \rho \cos \varphi \hat{k}$.

Next, we introduce a small parameter, ε , to study the dynamics when $\varphi = O(\varepsilon)$:

Proposition 3.5. *The reduced dynamics on the open set $\varphi = O(\varepsilon)$ may be reparametrized as the Hamiltonian flow of:*

$$\hat{F}_{red} = Kep_{\varepsilon^2} + Per, \quad \hat{\omega} = d\hat{L} \wedge d\hat{\ell} + d\hat{G} \wedge d\hat{g}$$

where $Kep_{\varepsilon^2} = -\frac{m^3}{2\hat{L}^2} + \frac{\varepsilon^2 \hat{L}^2}{2m}$, $m = m_1 m_2$, and $Per = \varepsilon^2 \left(\frac{\hat{C}^2}{2} - \hat{G}^2 + (m_2 - m_1)O(\varepsilon) + O(\varepsilon^2) \right)$.

Proof. Take Delaunay coordinates (prop. A.5), (L, G, ℓ, g) , for the Kep_κ term of F_{red} . Let $L^2 =: \rho \varepsilon \hat{L}^2, G^2 =: \rho \varepsilon \hat{G}^2, \|\vec{C}\|^2 =: \rho \varepsilon \hat{C}^2$, which imply $\varphi = O(\varepsilon)$. The dynamics of $\hat{F}_{red} := \rho \varepsilon F_{red}$ with symplectic form $\hat{\omega} := d\hat{L} \wedge d\hat{\ell} + d\hat{G} \wedge d\hat{g} = \omega / \sqrt{\rho \varepsilon}$, corresponds to the time reparametrization: $(\rho \varepsilon)^{3/2} \hat{t} = t$, where \hat{t} is the new time. Note that the mean anomaly, $\hat{\ell}$, for Kep_{ε^2} is the same as the mean anomaly, ℓ , for the Kep_κ term, as can be easily checked by comparing $d\ell = \partial_L Kep_\kappa dt$ and $d\hat{\ell} = \partial_{\hat{L}} Kep_{\varepsilon^2} d\hat{t}$. □

Remark 3.6. The scaling above includes the possibility of taking $\varepsilon = 1/\rho$, and in place of imagining the bodies as close, view their distance remaining bounded as the curvature of the space goes to zero.

Remark 3.7. When the curvature is negative, eq. (2) has the trigonometric functions replaced by their hyperbolic counterparts, and with $\mathfrak{so}_{2,1}^*$'s coadjoint orbits: $\nu_1^2 + \nu_2^2 - \nu_3^2 = \|\vec{C}\|_{2,1}^2$ replacing the coadjoint orbits of \mathfrak{so}_3^* . One arrives at $\hat{F}_{red} = Kep_{-\varepsilon^2} + \varepsilon^2 \left(\frac{\|\hat{C}\|_{2,1}^2}{2} + \hat{G}^2 + (m_2 - m_1)O(\varepsilon) + O(\varepsilon^2) \right)$.

4 Secular dynamics

By the *secular* or averaged dynamics we refer to the dynamics of the Hamiltonian:

$$\langle \hat{F}_{red} \rangle := \frac{1}{2\pi} \int_0^{2\pi} \hat{F}_{red} d\ell.$$

The secular dynamics admits \hat{L} as a first integral. We will use the brackets to denote a functions average over ℓ , namely $\langle f \rangle = \frac{1}{2\pi} \int_0^{2\pi} f d\ell$. The dynamical relevance of the secular Hamiltonian is due to its appearance in a series of 'integrable normal forms' for the reduced curved 2-body dynamics:

Proposition 4.1. *Consider the scaled Hamiltonian, $(\hat{F}_{red}, \hat{\omega})$, of proposition 3.5. For each $k \in \mathbb{N}$, there is a symplectic change of coordinates, $(\psi^k)^* \hat{\omega} = \hat{\omega}$, with:*

$$\hat{F}_{red} \circ \psi^k = Kep_{\varepsilon^2} + \langle Per \rangle + \langle F^1 \rangle + \dots + \langle F^{k-1} \rangle + F^k$$

and each $F^j = O(\varepsilon^{2j+3})$. When the masses are equal, $F^j = O(\varepsilon^{2j+4})$.

Proof. The iterative process to determine the sequence of ψ^k and F^k 's is not new (see e.g. [9]). For the first step, let ψ^1 be the time 1-flow of a 'to be determined' Hamiltonian χ . By Taylor's theorem:

$$\hat{F}_{red} \circ \psi^1 = Kep_{\varepsilon^2} + Per + \{Kep_{\varepsilon^2}, \chi\} + \{Per, \chi\} + \int_0^1 (1-t) \frac{d^2}{dt^2} (\hat{F}_{red} \circ \psi^t) dt.$$

Let $\tilde{Per} := Per - \langle Per \rangle$. Note that, while $Per = O(\varepsilon^2)$, we have $\tilde{Per} = O(\varepsilon^3)$. Taking $\hat{n}\chi := \int_0^\ell \tilde{Per}(\hat{L}, l, \hat{G}, g) dl$, where $\hat{n} = \partial_{\hat{L}} Kep_{\varepsilon^2}$, we have:

$$Per + \{Kep_{\varepsilon^2}, \chi\} = \langle Per \rangle, \quad \chi = O(\varepsilon^3),$$

so that for ε sufficiently small ψ^1 is defined. Finally, integrating by parts, one has

$$F^1 := \{Per, \chi\} + \int_0^1 (1-t) \frac{d^2}{dt^2} (\hat{F}_{red} \circ \psi^t) dt = \int_0^1 \{\langle Per \rangle + t\tilde{Per}, \chi\} \circ \psi^t dt = O(\varepsilon^5).$$

This process may be iterated to obtain the sequence in the proposition. \square

Remark 4.2. The truncated, or k 'th order secular system: $Sec^k := Kep_{\varepsilon^2} + \langle Per \rangle + \langle F^1 \rangle + \dots + \langle F^{k-1} \rangle$ admits \hat{L} as an additional first integral, since it does not depend on ℓ . For each fixed k , the k 'th order secular system approximates the true motion over long time scales in a region of configurations with the 2-bodies sufficiently close. In appendix B, we compute an expansion, eq. (12), of $\langle Per \rangle$ in powers of ε to observe some finer descriptions of these orbits behaviour (see fig. 7 and rem. B.2).

By ignoring the $O(\varphi)$ terms in F_{red} , we have: $\dot{G} = 0$, $\dot{g} = -2\kappa G$, i.e. the Keplerian orbits experience precession (see fig. 4). We next will check that for φ sufficiently small, many such orbits survive the perturbation of including these $O(\varphi)$ terms: they may be continued to orbits of the reduced curved 2-body problem and then lifted to orbits of the curved 2-body problem.

4.1 Continued orbits

Applying a KAM theorem from [11], establishes certain quasi-periodic motions of the reduced problem. Introducing some notation, for $\gamma > 0, \tau > 1$, let

$$D_{\gamma, \tau} := \{v \in \mathbf{R}^2 : |\mathbf{k} \cdot v| \geq \frac{\gamma}{(|k_1| + |k_2|)^\tau}, \forall \mathbf{k} = (k_1, k_2) \in \mathbf{Z}^2 \setminus \{0\}\}$$

be the (γ, τ) -Diophantine frequencies. Take

$$\hat{\mathbf{B}} := \{(\hat{L}, \hat{G}) : 0 < \hat{G} \leq \hat{L} < 1\}$$

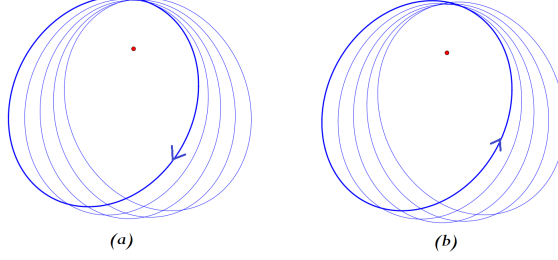


Figure 4: When the curvature is positive, (a), the Keplerian conic giving the particles relative motion precesses in a direction opposite to the particles (fast) motion around the conic. When the curvature is negative, (b), the precession occurs in the same direction as the particles motion.

and let

$$(I, \theta) = (I_1, I_2, \theta_1, \theta_2) = (\hat{L}, \hat{G}, \ell, g) + O(\varepsilon^3)$$

be action-angle variables for some k th order secular system, with $\mathbf{B} = \{(I_1, I_2) : (\hat{L}, \hat{G}) \in \hat{\mathbf{B}}\} \subset \mathbf{R}^2$ equipped with the Lebesgue measure, Leb , restricted to \mathbf{B} .

The reduced curved 2-body problem has, for φ sufficiently small, a positive measure of invariant tori along each of which the motions are quasi-periodic –behaving approximately as the precessing Keplerian orbits in fig. 4. More precisely:

Theorem 1. Fix $\tau > 1$, $\hat{\gamma} > 0$, $m > 2$ and set $\gamma := \varepsilon^m \hat{\gamma}$. There exists $\varepsilon_0 > 0$ such that for each $0 < \varepsilon < \varepsilon_0$, we have:

- (i) A positive measure set, $d_{\gamma, \tau} \subset \mathbf{B}$,
- (ii) for each $I^o \in d_{\gamma, \tau}$, there is a local symplectic change of coordinates, ψ^o , for which $\psi^o(I^o, \theta)$ is an invariant torus of \hat{F}_{red} with frequency in $D_{\gamma, \tau}$.
- (iii) As $\varepsilon \rightarrow 0$, $Leb(d_{\gamma, \tau}) \rightarrow Leb(\mathbf{B})$ and $\psi^o \rightarrow id$ (in the Whitney C^∞ topology).

Proof. We verify the hypotheses of [11]. Let (I, θ) be action-angle variables for a k 'th order secular system (remark 4.2) with $2k > 2m - 3$. Setting $s := I^o \in \mathbf{B}$, and $r := I - I^o$, we have by Taylor expansion:

$$F_s^o := Sec^k = c_s^o + \alpha_s^o \cdot r + O(r^2)$$

where $c_s^o := Sec_k(I^o)$, $\alpha_s^o := dSec^k(I^o)$. From the proof of proposition 4.1 ($\chi = O(\varepsilon^3)$), the action angle variables of Sec_k are $O(\varepsilon^3)$ close to those of proposition 3.5, so that:

$$\alpha_s^o = \left(\frac{m^3}{(I_1^o)^3} + \varepsilon^2 \frac{I_1^o}{m}, -2\varepsilon^2 I_2^o \right) + O(\varepsilon^3) = (O(1), O(\varepsilon^2)).$$

Note that for $0 < \varepsilon$ sufficiently small, α_s^o satisfies the non-degeneracy condition of being a *skew map*: its image is not contained in any 1-dimensional subspace of \mathbf{R}^2 .

Likewise, we take $F_s := \hat{F}_{red}(r, \theta)$ around $s = I^o$. Since we have chosen $2k + 1 > 2m$, we have:

$$|F_s - F_s^o| = o(\gamma^2)$$

for ε sufficiently small. So ([11] Thm. 15 and remark 21) there exists a map $\mathbf{B} \ni s \mapsto \alpha_s \in \mathbf{R}^2$, with $|\alpha_s - \alpha_s^o| \ll 1$ in the C^∞ -Whitney topology such that provided $\alpha_s \in D_{\gamma, \tau}$, we have $\hat{F}_{red} \circ \psi^o = c_s + \alpha_s \cdot r + O(r^2; \theta)$ for some local symplectic map ψ^o . It remains to check that $d_{\gamma, \tau} := \{s : \alpha_s \in D_{\gamma, \tau}\}$ is non-empty. Since $m > 2$ and $\alpha_s = (O(1), O(\varepsilon^2))$ is also skew, we have the estimate ([11] Cor. 29, from [13]):

$$Leb(\mathbf{B} \setminus d_{\gamma, \tau}) = O(\varepsilon^{\frac{m-2}{\mu}})$$

for some constant $\mu > 0$. So indeed, for ε sufficiently small, $d_{\gamma, \tau}$ has positive measure and is non-empty. \square

Remark 4.3. As the reduced dynamics has two degrees of freedom, there is KAM-stability in the $\varphi \ll 1$ regime: the invariant tori form barriers in energy level sets.

One may also apply the implicit function theorem to establish periodic orbits of long periods for the reduced dynamics:

Theorem 2. *Let $m, n \in \mathbb{N}$. Then for m sufficiently large, there exist periodic orbits of the reduced curved 2-body problem for which the bodies revolve m -times about their osculating conic, while the osculating conic precesses n -times around.*

Proof. We will consider non-equal masses, a similar argument applies for equal masses. After iso-energetic reduction, the equations of motion for \hat{G}, g are (from eq. (12)):

$$\frac{d\hat{G}}{d\ell} = \varepsilon^3 \Omega \sin g + O(\varepsilon^4), \quad \frac{dg}{d\ell} = -2\varepsilon^2 \hat{G} + O(\varepsilon^3),$$

where $\Omega(\hat{L}, \hat{G}) \neq 0$ for $|\hat{G}| \neq 0, \hat{L}, \hat{C}$. Consider the 'long time return map':

$$\bar{P}_\varepsilon(G^o, g^o) := \int_0^{2\pi/\varepsilon^2} \left(\frac{1}{\varepsilon} \frac{d\hat{G}}{d\ell}, \frac{dg}{d\ell} \right) d\ell,$$

the integral taken over an orbit with initial condition G^o, g^o . When $\bar{P}_\varepsilon(G^o, g^o) = (0, -2\pi n)$ and $1/\varepsilon^2 = m \in \mathbb{N}$, we have a periodic orbit as described in the theorem. The map \bar{P}_ε is analytic in ε , with

$$\bar{P}_0(G^o, g^o) = 2\pi(\Omega \sin g^o, -2G^o).$$

By the implicit function theorem, $g^o \equiv 0 \pmod{\pi}, G^o = \frac{n}{2}$, continues to solutions of $\bar{P}_\varepsilon(G^\varepsilon, g^\varepsilon) = (0, -2\pi n)$ for $0 < \varepsilon < \varepsilon_o$, yielding periodic orbits of long periods for those ε with $1/\varepsilon^2 = m \in \mathbb{N}$. \square

Remark 4.4. When the curvature is positive the precession is, as with the quasi-periodic motions, in the opposite direction to the particles motion around the conic, while for negative curvature in the same direction.

4.2 Lifted orbits

The continued orbits are the image under a near identity symplectic transformation of certain orbits of F_{red} with the $O(\varphi)$ terms neglected:

$$H_{red} := Kep_\kappa + \kappa \left(\frac{\|\vec{C}\|^2}{2} - G^2 \right). \quad (4)$$

We describe how the precessing Keplerian orbits of (4) lift to T^*Q . Recall our coordinates, eq. (3), used for the co-adjoint orbits. We have: $Ad_g^*(\nu_1, \nu_2, \nu_3) = g^t(\nu_1, \nu_2, \nu_3)$, and take $G = p_\theta$. Let us set $\mu_o = (0, 0, \|\vec{C}\|)$, corresponding to an angular momentum vector along the \hat{k} -axis.

Then, in the reduced space, $T^*I \times \mathcal{O}_{\mu_o}$, the orbits of (4) are given by:

$$(\varphi(t), p_\varphi(t), Ad_{g(t)}^* \mu_o)$$

where $g(t) = R_{\hat{i}}(\lambda)R_{\hat{k}}(\theta(t))$ is a rotation by $\theta(t)$ about the \hat{k} -axis followed by a rotation by λ about the \hat{i} -axis. Moreover, $(\varphi(t), \theta(t))$ describe a precessing orbit of the curved Kepler problem (fig. 4) having angular momentum

$$G = \|\vec{C}\| \cos \lambda.$$

Since $\vec{C} = \|\vec{C}\|\hat{k}$, the isotropy is by rotations about the \hat{k} -axis. The ambiguity in the reduced orbit is by $Ad_{g(t)}^* Ad_{h(t)}^* \mu_o$, where $h(t) = R_{\hat{k}}(\omega(t))$. Hence the lifted orbit, on T^*Q , is of the form:

$$(*) \quad (\varphi(t), p_\varphi(t), h(t)g(t), \mu_o).$$

Such an orbit's projection to Q , is the motion:

$$R_{\hat{k}}(\omega(t))R_{\hat{i}}(\lambda)R_{\hat{k}}(\theta(t))q^o(\varphi(t)),$$

as depicted in fig. 1, provided we show $\dot{\omega} > 0$. Indeed, the Hamiltonian (4) is the symplectic reduction of H on T^*Q given by $H(\varphi, p_\varphi, g, \mu) = H_{red}(\varphi, p_\varphi, Ad_g^*\mu)$. Requiring the lifted curve (*) to satisfy the equations of motion of H , imposes the condition:

$$\dot{\omega} = \kappa \|\vec{C}\|.$$

In summary, a precessing Keplerian orbit of (4) with angular momentum G lifts to a curve with angular momentum μ_o on T^*Q , projecting to an orbit in Q where the two bodies follow precessing Keplerian orbits with foci on the colatitude, λ , satisfying $\|\vec{C}\| \cos \lambda = G$. The whole system is uniformly rotated with angular speed $\kappa \|\vec{C}\|$ about the \hat{k} axis.

Remark 4.5. The collision orbits, $G = 0, g \equiv \theta^o - \pi$, of (4) lift to collision orbits,

$$R_{\hat{k}}(\omega(t)) R_{\hat{i}}\left(\frac{\pi}{2}\right) R_{\hat{k}}(\theta^o) q^o(\varphi(t)),$$

centered on the 'equator', \vec{C}^\perp , experiencing no precession (see remark B.2, for some effects of the $O(\varphi)$ terms on the true behaviour near collisions). There are 3 parameters involved in describing the lifted orbits we consider of (4), namely G, L , and $C := \|\vec{C}\|$, where G, L are the Delaunay coordinates (for non-circular motions $|G| < L$) and for the circular motion, when $G = L$, one should take Poincaré coordinates (prop. A.5). The well-known circular relative equilibrium solution corresponds to when $G = L = C$. When $C > L \geq G$, the lifted orbits are constrained to bands, $\cos \lambda \leq \frac{L}{C} < 1$, around the equator, at an extremal value, λ_c , of λ , we have a circular motion whose center moves along the latitude λ_c at the constant rate κC . For $L > C$, one obtains with $G = C$ a precessing non-circular motion having a focus over \hat{k} .

The true motions of the reduced curved 2-body problem established in the previous section lift to orbits which are qualitatively the same as such lifted orbits of (4), performing small oscillations around them.

A Action-angle coordinates for the curved Kepler problem

A.1 Curved conics

The Kepler problem on a sphere of radius ρ with a fixed 'sun', q_s , of mass M and particle, $q \in S^2$, of mass m is given by the Hamiltonian flow of:

$$Kep_\kappa := \frac{\|p\|_\kappa^2}{2m} - \frac{mM}{\rho} \cot \varphi$$

on $T^*(S^2 \setminus \{|\cot \varphi| = \infty\})$. Here $\|\cdot\|_\kappa$ is the norm induced by the metric of constant curvature $\kappa = 1/\rho^2$ on S^2 and φ is the angular distance from q_s to q (see figure 2). For a negatively curved space, one replaces $\cot \varphi$ with $\coth \varphi$.

Because the force is central, letting $\vec{q} \in \mathbf{R}^3$ be the position of the particle from the center, c , of the sphere and \hat{k} a unit vector from c to q_s , the *angular momentum*:

$$G := m(\vec{q} \times \dot{\vec{q}}) \cdot \hat{k}$$

is a first integral. It corresponds to the rotational symmetry about the $c\vec{q}_s$ axis.

Remark A.1. In spherical coordinates, $\vec{q} = \rho(\sin \varphi \cos \theta, \sin \varphi \sin \theta, \cos \varphi)$, we have: $\|p\|_\kappa^2 = \frac{1}{\rho^2}(p_\varphi^2 + \frac{p_\theta^2}{\sin^2 \varphi})$, and $G = m\rho^2 \sin^2 \varphi \dot{\theta} = p_\theta$. In these coordinates, it is not hard to show analytically that the curved Kepler trajectories centrally project to flat Kepler orbits (fig. 2). Indeed, setting $R = 1/r := \frac{\cot \varphi}{\rho}$, one finds $\frac{d^2 R}{d\theta^2} + R = m^2 M / G^2$, so that the θ -parametrized orbits are: $r = \frac{G^2 / m^2 M}{1 + e \cos(\theta - g)}$, with e and g being constants of integration. Here $\nu := \theta - g$ is the true anomaly and g is the *argument of pericenter*.

The curved Kepler trajectories are in fact conic sections on the sphere having a focus at q_s (see fig. 5). One may express energy and momentum in terms of geometric parameters of such spherical conics.

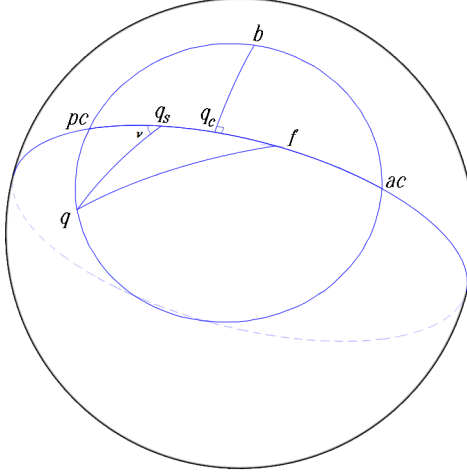


Figure 5: A spherical ellipse, with foci at q_s and f is the set of points q for which $|qq_s| + |qf| = 2\alpha$ is constant. We call α its *semi-major axis*, the midpoint, q_c , between the foci its *center*, and the length $|bq_c| =: \beta$ its *semi-minor axis*. The number, ϵ , for which $|q_sq_c| = \alpha\epsilon$ is called the *eccentricity*. When $\epsilon \neq 0$, the closest point to q_s is called the *pericenter*, pc , and furthest, ac , the *apocenter*. The angle $\nu := \angle(pc, q_s, q)$ is called the *true anomaly* of q .

Proposition A.2. Consider an orbit of the curved Kepler problem along a spherical conic with a focus at q_s (fig. 5). Let α be the semi-major axis and β the semi-minor axis of this conic. The orbit has energy and momentum:

$$Kep_\kappa = -\frac{mM}{\rho} \cot \frac{2\alpha}{\rho},$$

$$G^2 = m^2 M \rho \tan^2 \frac{\beta}{\rho} \cot \frac{\alpha}{\rho}.$$

Proof. Consider the spherical triangle $\Delta(f, q_s, q)$ with sidelengths $2\alpha\epsilon, \rho\varphi, 2\alpha - \rho\varphi$ and interior angle $\pi - \nu$ opposite to side fq (see fig. 5). The cosine rule of spherical trigonometry yields: $r = \rho \tan \varphi = \frac{p^2}{1+e \cos \nu}$, where $p^2 = \rho \frac{\cos \frac{2\alpha\epsilon}{\rho} - \cos \frac{2\alpha}{\rho}}{\sin \frac{2\alpha}{\rho}}$ and $e = \frac{\sin \frac{2\alpha\epsilon}{\rho}}{\sin \frac{2\alpha}{\rho}}$, so that the orbits are indeed curved conic sections. Comparing with the expression in remark A.1 yields $G^2 = m^2 M p^2$. The expression for G in the proposition follows by using the relation: $\cos \frac{\beta}{\rho} = \frac{\cos \frac{\alpha}{\rho}}{\cos \frac{\alpha\epsilon}{\rho}}$ (consider the right spherical triangle $\Delta(q_s, q_c, b)$), to simplify.

To obtain the expression for Kep_κ , following [1], observe that $\varphi_p := \frac{\alpha(1-\epsilon)}{\rho}$ and $\varphi_a := \frac{\alpha(1+\epsilon)}{\rho}$ are maximal and minimal values of φ over the trajectory having energy $Kep_\kappa =: h$. Consequently $p_\varphi = 0$ at $\varphi_{a,p}$ so we have two solutions of the equation: $h \cos 2\varphi = \frac{mM}{\rho} \sin 2\varphi + h - \frac{G^2}{\rho^2}$. Adding and subtracting the above equation evaluated at $\varphi_{a,p}$ yields: $Kep_\kappa = h = \frac{mM}{\rho} \frac{\sin 2\varphi_a - \sin 2\varphi_p}{\cos 2\varphi_a - \cos 2\varphi_p} = -\frac{mM}{\rho} \cot(\varphi_a + \varphi_p)$. \square

Remark A.3. The sign of G represents the orbits orientation, with positive G for counterclockwise motion around q_s . The same arguments apply to bounded motions when the curvature is negative, replacing trigonometric functions with their hyperbolic counterparts. The energy for bounded motions in a space of curvature $\kappa = -1/\rho^2$ is always less than $-mM/\rho$.

Remark A.4. The orbits of the curved Kepler problem colliding with q_s may be regularized similarly to the usual Kepler regularization, via an elastic bounce [2].

A.2 Delaunay and Poincaré coordinates

We have the following analogues of the Delaunay and Poincaré symplectic coordinates for the bounded motions of the curved Kepler problem. Note that to each point of $p \in T^*(S^2 \setminus \{\pm q_s\})$, one may associate a pointed spherical conic and conversely, parametrizations of pointed conics may serve as local coordinates for $T^*(S^2 \setminus \{\pm q_s\})$.

Proposition A.5. *Given a pointed spherical conic (fig. 5), let G be its angular momentum, g its argument of pericenter,*

$$L^2 := m^2 M \rho \tan \frac{\alpha}{\rho}, \quad L > 0,$$

and ℓ , the mean anomaly, be proportional to time along the conic to pericenter, scaled so that $\ell \in \mathbf{R}/2\pi\mathbf{Z}$. Then (L, ℓ, G, g) are symplectic (Delaunay) coordinates for bounded non-circular motions. The variables:

$$\Lambda = L, \quad \lambda = \ell + g, \quad \xi = \sqrt{2(L - |G|)} \cos g, \quad \eta = \sqrt{2(L - |G|)} \sin g,$$

are symplectic (Poincaré) coordinates in a neighborhood of the circular motions. The energy is given by:

$$Kep_\kappa = -\frac{m^3 M^2}{2L^2} + \kappa \frac{L^2}{2m}. \quad (5)$$

Proof. The construction of these coordinates is almost identical as for the planar Kepler problem (see e.g. the presentation in [10]). We only found some difference in the computation determining L owing to, in the curved case, the period as a function of energy (Kepler's third law) not having such a simple expression.

For non-circular motions, we have symplectic coordinates $(H = Kep_\kappa, t, G, g)$, where t is the time along the orbit (to pericenter). Since orbits of fixed energy, $Kep_\kappa = H$, all have a common period, $T(H)$, we set $\ell = \frac{2\pi}{T(H)}t$ and seek a conjugate coordinate $L(H)$ to ℓ , i.e. we want to integrate:

$$dL = \frac{T(H)}{2\pi} dH.$$

To integrate this expression, we make some changes of variable. For H a negative energy value admitting bounded motions, let $\varphi_c(H)$ be the angular distance of the circular orbit having energy H . Then:

$$H = -\frac{mM}{\rho} \cot 2\varphi_c, \quad G_c T(H) = 2\pi m \rho^2 \sin^2 \varphi_c$$

where $G_c^2 := \rho m^2 M \tan \varphi_c$ is the angular momentum of the circular solution. Note that

$$(*) \quad H = -\frac{m^3 M^2}{2G_c^2} + \kappa \frac{G_c^2}{2m}.$$

We compute $\frac{T}{2\pi} dH = dG_c$. So we take $L = G_c$, and have $L^2 = m^2 M \rho \tan \frac{\alpha}{\rho}$ from $(*)$ and prop. A.2. \square

Remark A.6. The *mean anomaly*, ℓ , is related to time by $d\ell = n dt$ where $n(L) := \frac{m^3 M^2}{L^3} + \kappa \frac{L}{m}$. When the curvature is negative, the same arguments lead to $L^2 = m^2 M \rho \tanh \frac{\alpha}{\rho}$, and the same expression, eq. (5), for the energy.

A.3 Other anomalies

In averaging functions over curved Keplerian orbits, i.e. determining $\frac{1}{2\pi} \int_0^{2\pi} f(q) d\ell$, it is often useful to perform a change of variables, as the position on the orbit, q , does not have closed form expressions in terms of ℓ . We collect here some parametrizations of Keplerian orbits. Although not all are necessary for our main results, they may serve useful in other perturbative studies of the curved Kepler problem.

The position on the conic is given explicitly in terms of the true anomaly (remark A.1). By conservation of angular momentum (recall $d\ell = n dt$ with $n = \frac{m^3 M^2}{L^3} + \kappa \frac{L}{m}$):

$$G d\ell = n m \rho^2 \sin^2 \varphi d\nu.$$

One may centrally project a curved Kepler conic to the tangent plane at q_s and then parametrize this planar conic by its eccentric anomaly, which we denote here by u_o . Letting a, e, b be the semi-major axis, eccentricity and minor axis of this planar conic, the position is given by:

$$r = \rho \tan \varphi = a(1 - e \cos u_o) \quad x = r \cos \nu = a(\cos u_o - e) \quad y = r \sin \nu = b \sin u_o \quad (6)$$

and one has:

$$\sqrt{\frac{M}{a}} d\ell = n \rho \sin \varphi \cos \varphi du_o. \quad (7)$$

Some more parametrizations arise naturally when one *orthogonally* projects the curved Kepler ellipse onto the tangent plane at q_s . The time-parametrized motion along this plane curve sweeps out area at a constant rate, however it is now a quartic curve: the locus of a 4th order polynomial in the plane. This quartic may be seen naturally as an elliptic curve and then parametrized by Jacobi elliptic functions. Taking $R = \rho \sin \varphi, X = R \cos \nu, Y = R \sin \nu$, the quartic is the projection to the XY -plane of the intersection of the quadratic surfaces:

$$R^2 = X^2 + Y^2, \quad (R + eX)^2 = p^2(1 - \kappa R^2),$$

where p, e are as in the proof of prop. A.2. Consequently we find the parametrization:

$$R = \rho \sin \frac{\alpha}{\rho} k' \text{nd}_k w - \rho \cos \frac{\alpha}{\rho} k \text{cd}_k w \quad X = \rho \sin \frac{\alpha}{\rho} k' \text{cd}_k w - \rho \cos \frac{\alpha}{\rho} k \text{nd}_k w \quad Y = \rho \tan \frac{\beta}{\rho} \cos \frac{\alpha}{\rho} \text{sd}_k w.$$

where $k = \sin \frac{\alpha \epsilon}{\rho}, k' = \cos \frac{\alpha \epsilon}{\rho}$. Since the area is swept at a constant rate, one computes:

$$\rho \sin \frac{\alpha}{\rho} d\ell = \rho \sin \varphi dw.$$

which integrates to give a 'curved Kepler equation', i.e. the relation between position and time through:

$$\ell = \arccos \text{cd}_k w - \frac{\cot \frac{\alpha}{\rho}}{2} \log \frac{1 + k \text{sn}_k w}{1 - k \text{sn}_k w} \quad (8)$$

It turns out that a geometric definition of eccentric anomaly, u (see fig. 6), is the Jacobi amplitude of w :

$$du = d\text{n}_k w dw,$$

which can be established by using spherical trigonometry to give the position in terms of u , and some straightforward, although tedious, simplification.

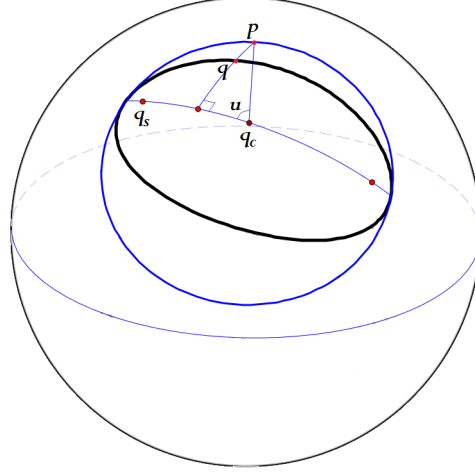


Figure 6: A 'curved eccentric anomaly', u , for a (non-circular) Keplerian conic on the sphere. One circumscribes a (spherical) circle centered at q_c around the conic and to a point q on the conic assigns the angle $u := \angle(p_c, q_c, p)$, where p is the intersection of the circle with the perpendicular dropped from q to the major axis.

Remark A.7. Projecting the spherical orbits from the south pole leads as well to quartic curves in the tangent plane at q_s , however along these quartics the time-parametrization is no longer by sweeping area at a constant rate –as it is for orthogonal projection– which we found only led to complicated expressions. Another parametrization of the orbits is presented in [12] eq. (28), and used to derive a different 'curved Kepler equation' from our eq. (8).

B Expansion of $\langle Per \rangle$

We will compute an expansion, eq. (12), in powers of our small parameter ε for $\langle Per \rangle$ (prop. 3.5) upto $O(\varepsilon^5)$. This expansion may be found by using the 'flat eccentric anomaly', u_o , of eq. (7) to average the terms. With this approach, it is necessary to make use of the following formulas allowing one to translate between the major axis and eccentricity (a, e) of the centrally projected planar conic and our Delaunay coordinates:

$$a = \frac{L^2}{m^2} \left(\frac{1}{1 - \frac{\kappa}{m^4} L^2 (L^2 - G^2)} \right) = \rho \varepsilon \frac{\hat{L}^2}{m^2} (1 + O(\varepsilon^2)), \quad e^2 = (1 - \frac{\hat{G}^2}{\hat{L}^2}) (1 + \frac{\varepsilon^2}{m^4} \hat{L}^2 \hat{G}^2)$$

(recall we set $m = m_1 m_2$). Note that by eq. (6), $r = \rho \tan \varphi = \rho O(\varepsilon)$, so indeed $\varphi = \frac{r}{\rho} + O(\varepsilon^3)$ is $O(\varepsilon)$.

By Taylor expansion of eq. (2) in φ , and then exchanging φ to $\frac{r}{\rho}$, we have:

$$Per = \varepsilon^2 \left(\frac{\hat{C}^2}{2} - \hat{G}^2 + \frac{2}{3} (m_2 - m_1) \hat{G} \sqrt{\hat{C}^2 - \hat{G}^2} \frac{r \cos \theta}{\rho} + ((\hat{C}^2 - \hat{G}^2) \cos^2 \theta - \hat{G}^2) \sigma \frac{r^2}{\rho^2} \right) + O(\varepsilon^5), \quad (9)$$

where we set $\sigma = \frac{1 - (m_1^3 + m_2^3)}{6}$. So, to determine $\langle Per \rangle = \frac{1}{2\pi} \int_0^{2\pi} Per d\ell$ upto $O(\varepsilon^5)$, it remains to find:

$$\langle r \cos \theta \rangle, \quad \langle r^2 \cos^2 \theta \rangle, \quad \langle r^2 \rangle.$$

By eq. (7), $d\ell = n \sqrt{a} \frac{r}{1 + \kappa r^2} du_o = n \sqrt{a} r (1 - \kappa r^2 + O(\varepsilon^4)) du_o$, where

$$n \sqrt{a} = \frac{m^2}{\rho \varepsilon \hat{L}^2} + O(\varepsilon).$$

Hence:

$$\langle r \cos \theta \rangle = \frac{n \sqrt{a}}{2\pi} \int_0^{2\pi} r^2 \cos \theta - \kappa r^3 \cos \theta du_o + O(\varepsilon^3).$$

Using $\theta = \nu + g$, and the expressions for $r, r \cos \nu, r \sin \nu$ of eq. (6), we obtain:

$$\langle r \cos \theta \rangle = a^2 e n \sqrt{a} \cos g \left(-\frac{3}{2} + \kappa a (2 + \frac{e^2}{2}) \right) + O(\varepsilon^3).$$

Or, in terms of the (scaled) Delaunay coordinates:

$$\langle r \cos \theta \rangle = \rho \varepsilon \cos g \hat{L} \sqrt{\hat{L}^2 - \hat{G}^2} \left(-\frac{3}{2} + \frac{\varepsilon}{2\rho m^2} (5\hat{L}^2 - 3\hat{G}^2) \right) + O(\varepsilon^3). \quad (10)$$

Likewise, one computes:

$$\langle r^2 \cos^2 \theta \rangle = \frac{\rho^2 \varepsilon^2}{2m^4} \hat{L}^2 \left(2\hat{L}^2 + (3 + 5 \cos 2g)(\hat{L}^2 - \hat{G}^2) \right) + O(\varepsilon^4), \quad \langle r^2 \rangle = \frac{\rho^2 \varepsilon^2}{2m^4} \hat{L}^2 (5\hat{L}^2 - 3\hat{G}^2) + O(\varepsilon^4). \quad (11)$$

Combining eqs. (10), (11) with the averaged eq. (9), yields:

$$\begin{aligned} \langle Per \rangle &= \varepsilon^2 \left(\frac{\hat{C}^2}{2} - \hat{G}^2 \right) + \varepsilon^3 \left(m_\Delta \hat{L} \hat{G} \sqrt{(\hat{C}^2 - \hat{G}^2)(\hat{L}^2 - \hat{G}^2)} \cos g \right) \\ &\quad + \varepsilon^4 \left[\tilde{m} \hat{L}^2 \left((\hat{C}^2 - \hat{G}^2)(2\hat{L}^2 + (\hat{L}^2 - \hat{G}^2)(3 + 5 \cos 2g)) - \hat{G}^2 (5\hat{L}^2 - 3\hat{G}^2) \right) \right. \\ &\quad \left. - \frac{m_\Delta}{3\rho m^2} \hat{L} \hat{G} \sqrt{(\hat{L}^2 - \hat{G}^2)(\hat{C}^2 - \hat{G}^2)} (5\hat{L}^2 - 3\hat{G}^2) \cos g \right] + O(\varepsilon^5), \end{aligned} \quad (12)$$

where we set $m_\Delta = m_1 - m_2$, $\tilde{m} = \frac{1 - m_1^3 - m_2^3}{12m^4}$, and $m = m_1 m_2$.

Remark B.1. When the masses are equal, one may avoid the need to take expansions as we have done here by using the simplified expression in remark 3.3, and making use of the different anomalies presented in section A.3 to obtain explicit, albeit still rather complicated, expressions.

In the secular dynamics, we may view \hat{L}, \hat{C} as parameters, and then describe the dynamics of non-circular motions in the coordinates (\hat{G}, g) . To see the behaviour near circular motions (when $\hat{G} = \hat{L} \leq \hat{C}$), one may convert eq. (12) to Poincaré coordinates, in which one finds the circular motion is an elliptic fixed point. Taking into account higher order terms of $\langle Per \rangle$ leads to finer descriptions of the orbits. For example above we have for the most part worked at order ε^2 , when we see the precession properties described for our continued orbits. In fig. 7, we plot some level curves of eq. (12).

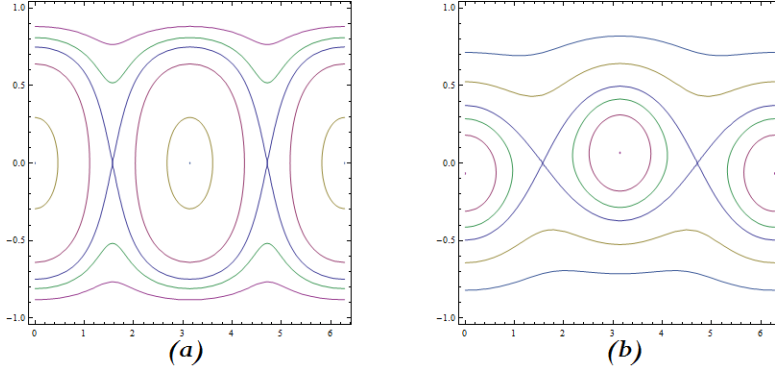


Figure 7: Level sets of $\langle Per \rangle$, with $\hat{L} = \hat{C} = 1$. The vertical axis is the angular momentum, $\hat{G} \in [-1, 1]$, and the horizontal axis the argument of pericenter, $g \in [0, 2\pi]$. In (a), we have equal masses, while in (b) non-equal masses. The two stable circular orbits are, in these coordinates, blown up to the lines $\hat{G} = \pm 1$.

Remark B.2. The equilibrium points, $G = 0, 2g \equiv 0 \bmod \pi$ for equal masses, in fig. 7(a) correspond to (regularized) periodic collision orbits of the reduced dynamics (for non-equal masses, one has high eccentricity ‘near collision orbits’).

According to remark 4.5, the stable (elliptic) points, $g = 0, \pi$, lift to collision orbits bouncing perpendicularly to the equator, \vec{C}^\perp (depicted in fig. 1). The closed curves surrounding these stable points represent invariant (punctured) tori of the reduced dynamics different than those described above as, rather than precessing at a constant rate, the osculating conics experience libration: with g oscillating around π or zero.

The unstable (hyperbolic) points, $g = \frac{\pi}{2}, \frac{3\pi}{2}$, lift to collision orbits bouncing along an arc aligned with the equator. In the true dynamics, one expects a splitting of the separatrices connecting these unstable orbits. Note that, by prop. 4.1, such a splitting would be exponentially small, i.e. of $O(\exp(-1/\varepsilon))$. If one could establish such a transversal intersection, one would obtain random motions near these unstable collision orbits admitting the following description. For any sequence s_0, s_1, \dots with $s_k \in \{0, 1\}$, there would exist a near collision orbit for which, during the time interval $[nT, (n+1)T]$ the osculating conic precesses s_n times around, and where $T > 0$ is some sufficiently long time period.

Acknowledgements

I thank Luis García-Naranjo, Gil Bor, and Ernesto Pérez-Chavela for helpful discussions, comments, and encouragement to pursue this project. Also, I would like to thank Jacques Féjoz for inspiring my interest in applications of averaging methods during the MSRI program “Hamiltonian systems, from topology to applications through analysis”. This work was supported through CIMAT and CONACyT.

References

- [1] A. Albouy, *There is a projective dynamics*. Eur. Math. Soc. Newslett., 89, 37-43 (2013).

- [2] J. Andrade, N. Dávila, E. Pérez-Chavela, C. Vidal, *Dynamics and regularization of the Kepler problem on surfaces of constant curvature*. Canadian Journal of Mathematics, 69(5), 961-991 (2017).
- [3] V. I. Arnold, *Mathematical methods of classical mechanics* (Vol. 60). Springer Science & Business Media, (2013).
- [4] A.V. Borisov, I.S. Mamaev, *The restricted two-body problem in constant curvature spaces*. Celestial Mechanics and Dynamical Astronomy, 96(1), 1-17 (2006).
- [5] A.V. Borisov, I.S. Mamaev, A.A. Kilin, *Two-body problem on a sphere. Reduction, stochasticity, periodic orbits*. Regular and chaotic dynamics, V. 9, no. 3, 265-279 (2004).
- [6] A.V. Borisov, I.S. Mamaev, I.A. Bizyaev, *The spatial problem of 2 bodies on a sphere. Reduction and stochasticity*. Regular and Chaotic Dynamics, 21(5), 556-580 (2016).
- [7] A. V. Borisov, L.C. García-Naranjo, I.S. Mamaev, J. Montaldi, *Reduction and relative equilibria for the two-body problem on spaces of constant curvature*. Celestial Mechanics and Dynamical Astronomy, 130(6), 43 (2018).
- [8] F. Diacu, E. Pérez-Chavela, M. Santoprete, *The n-body problem in spaces of constant curvature*. arXiv preprint arXiv:0807.1747 (2008).
- [9] J. Féjoz, *Quasiperiodic motions in the planar three-body problem*. Journal of Differential Equations, 183(2), 303-341 (2002).
- [10] J. Féjoz, *On action-angle coordinates and the Poincaré coordinates*. Regular and Chaotic Dynamics, 18(6), 703-718 (2013).
- [11] J. Féjoz, *Introduction to KAM theory, with a view to celestial mechanics*. Variational methods in imaging and geometric control Radon Series on Comput. and Applied Math. 18, de Gruyter, ed. J.-B. Caillau, M. Bergounioux, G. Peyré, C. Schnörr, T. Haberkorn (2016).
- [12] V.V.E. Kozlov, *Dynamics in spaces of constant curvature*. Vestnik Moskovskogo Universiteta. Seriya 1. Matematika. Mekhanika, (2), 28-35 (1994).
- [13] H. Rüssmann, *Invariant tori in non-degenerate nearly integrable Hamiltonian systems*. Regular and Chaotic Dynamics 6.2 (2001): 119-204.
- [14] A.V. Shchepetilov, *Nonintegrability of the two-body problem in constant curvature spaces*. Journal of Physics A: Mathematical and General, 39(20), 5787 (2006).